AIAA JOURNAL
Vol. 40, No. 6, June 2002

Influence of a Counterflow Plasma Jet on Supersonic Blunt-Body Pressures

V. M. Fomin* and A. A. Maslov†
Institute of Theoretical and Applied Mechanics, Novosibirsk, 630090, Russia
N. D. Malmuth‡
Rockwell Scientific Company, Thousand Oaks, California 91360
and
V. P. Fomichev,§ A. P. Shashkin,§ T. A. Korotaeva,§ A. N. Shiplyuk,§ and G. A. Pozdnyakov§
Institute of Theoretical and Applied Mechanics, Novosibirsk, 630090, Russia

Aerodynamic augmentation in the presence of a thin high-temperature onboard plasma jet directed upstream of a slightly blunted cone was studied experimentally and numerically. The flow around a truncated cone cylinder at zero incidence was considered for Mach numbers M_∞ = 2.0, 2.5, and 4.0. For the first time, computationally validated experimental pressure distributions over the model surface in the presence of the plasma jet were obtained. As in the conventional (nonplasma) counterflow jet, two stable operational regimes of the plasma jet were found. These were a short penetration mode and a long penetration mode (LPM) aerospike into the opposing supersonic freestream. The greatest drag reduction occurred in the moderate LPM regime. LPM strong overblowing reduces the benefits. The experimental pressure results were approximately validated against an Euler computational fluid dynamics simulation, modeling a perfect gas hot jet, counterflowing against a perfect gas supersonic freestream. Plasma effects such as electron pressure, radiation, electric field interactions, Joule heating, and induced vorticity, streamers, and plasmoids have been identified that, if accounted for, may improve the comparison. Procedures for the use of these experimental results have been outlined as a baseline that will be useful in separating fluid dynamic/thermal effects from plasma processes in understanding the physics of onboard plasma jets for aerodynamic augmentation.

Introduction

CONSIDERABLE interest exists today regarding the application of onboard plasma devices (OBPD) to enhance aerodynamic performance of flight vehicles. A number of concepts that have been considered include microwave, electron beams, surface and volume discharges such as coronas, and plasma jets. Both numerical and experimental papers devoted to this problem are exemplified in Refs. 1–5. The effect of a laser optical pulse discharge in a supersonic flow giving a spikelike energy source decreases conical and hemispherical nose drag.[6] Bodies of revolution with varying bluntness ranging from a sphere to a flat-faced cylinder were considered[3,4,7] for different methods of modifying the flow such as microwaves, heated wires, or glowing discharges.

Originally, much of the interest was stimulated by the possibility of weakening the vehicle shock system by the interaction of the artificially generated plasma with the shock system. One of our conjectures is that streamers form that create strong delta-function-like transverse temperature gradients. By Crocco's theorem, these create intense vorticity that can attenuate the shocks. The origin of the plasma aerodynamic augmentation or flow modification is quite controversial, with one camp believing that the major effects are due to heating and conventional fluid mechanics, whereas another is convinced that it is all due to plasma physics. Most likely, any benefits are due to a combination of both phenomena. The relative proportion of each is related to the device or scheme used to obtain aerodynamic benefits and the range of parameters considered.

How to create a power source using the minimum possible energy in these devices is not obvious now. Weight and size as well as scaling (including identification of the correct parameters) are key for systems integration and tradeoff comparisons against conventional thrust augmentation schemes for rocket and scramjet propelled vehicles. New databases and modeling are needed to deal with these issues. Thermodynamic analyses are also needed to bound the problem.

An example of a simple plasma aerodynamic augmentation device is a counterflow plasma jet. Experimental studies on injection of a cold ordinary gas jet were described in Refs. 8–11. The possibility of decreasing the drag of a blunted body was demonstrated in these studies,[12–14] including experiments and numerical modeling. This work was extended for hot and, later, plasma jets in Refs. 15 (by the authors; the forerunner of this paper), 16, and 17. Available data show that the jet effects substantially depend on the shape of the housing parent body as well as on the jet and freestream flow conditions. However, these data are scattered and do not lead to general conclusions.

Most of the OBPD literature gives information on overall forces and moments without providing pressure distributions. This information is the minimum needed to resolve the aforementioned controversy and is a central theme in this paper, which not only provides this information but also computational fluid dynamics (CFD) validations of perfect gas Euler simulations that can be used to test the hypothesis that, for a range of plasma parameter space, plasma effects such as electron pressure, electric fields, charge separation, plasma radiation, and nonequilibrium and vibrational relaxation are small compared to Joule heating source terms modifying a perfect gas simulation of the plasma jet flow modification. This study examines the conjecture that, if the flow patterns and pressures are approximately similar between experiment and an Euler computational model, conventional gasdynamic processes control the flow. Independent of its origin, heat addition significantly modifies the body flowfield, forming a complex system of compression and expansion waves interacting with bifurcational unsteady flow separations and

Presented as Paper 99-4883 at the AIAA 3rd Weakly Ionized Workshop, Norfolk, VA, 1–4 November 1999; received 11 January 2001; revision received 12 December 2001; accepted for publication 12 December 2001.

*Director.
†Deputy Director. Member AIAA.
‡Senior Scientist and Program Manager, Fluid Dynamics. Fellow AIAA.
§Senior Scientist.

cavities. These bifurcations produce significant changes in the body forces and moments.

Existing onboard plasma jet experimental databases contain no pressure distributions. Furthermore, no adequate theoretical model exists currently. To fill these gaps, experiments and modeling were performed. A description of these studies follows.

Test Facility and Equipment

Performance of counterflow plasma jets in supersonic freestreams was the primary focus of the experimental portion of the investigation. A significant capability was the availability of a long runtime Institute of Theoretical and Applied Mechanics T-325, Siberian Branch of the Russian Academy of Sciences supersonic wind tunnel for the counterflow plasma jet experiments. In this facility, the test section, which is $200 \times 200 \times 600$ mm, provided good views of the flow patterns. The long run times were ideally suited for understanding the flow patterns to be described.

Experiments were performed at Mach numbers $M_\infty = 2.0$, 2.5, and 4.0, total temperature 300 K, and stagnation pressures 1–3 atm, which correspond to unit Reynolds numbers $Re_1 = (13\text{–}40) \times 10^6$ 1/m.

The nonuniformity of the Mach number in the test section did not exceed $\pm 0.8\%$. Pressure and temperature in the settling chamber was measured and kept constant within an accuracy of $\pm 0.5\%$. The test article was a cylinder with a blunted cone forebody. The cone half-angle was $\Theta_c = 30$, and it was 40 mm in diameter and 200 mm in length. The cone was mounted in the wind-tunnel test section with a strut on one window, so that its forebody could be seen through the test section optical glass. The blunted cone nose was necessary to accommodate a nozzle for the plasma generator and to inject the plasma jet. Figure 1 shows the plasma generator nozzle located in the forebody of the model. A dc plasma generator with a variable length arc and gasdynamic displacement of the anode spot on the anode surface was used in the experiments. The discharge current was 30–60 A, voltage was 100–200 V, and the characteristic value of the power supply in the gas was 6 kW/g. A (continuous) plasma generator produced a hot jet of nitrogen of temperature 5000 K and gas flow rate 0.7 g/s. The body of the plasma generator was bounded by a water-cooling jacket that permitted long, continuous runs. Current, voltage, gas flow rate, and pressure in a prechamber of the plasma generator were measured in the experiments. The plasma generator operational parameters were adjusted before each T-325 wind-tunnel run. The flow conditions were monitored during the runs.

Standard equipment was used for measurements of current, voltage, and pressure. Precision of measurements of current and voltage was $\pm 0.5\%$ and pressure $\pm 3\%$, respectively.

The plasma generator was attached to a strut that did not affect the measured value of the model drag. The metric part of the model was a thin-walled shell that was attached to a strain-gauge balance located on the extreme downstream end of the casing shield. A strain-gauge registered forces acting only on the thin-walled shell. The forces acting on the plasma generator (including the jet reaction force) were compensated by the strut response that was not measured by the balance.

On the forebody of the model, 10 pressure taps were installed, and 6 were placed on the cylindrical afterbody. Three pressure sensors were located inside the model, between the cone and plasma generator. One was located near the strain-gauge balance.

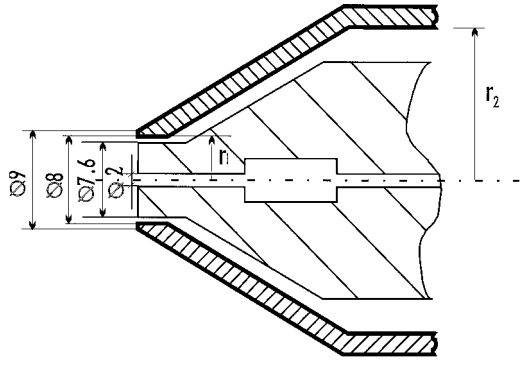

Fig. 1 Plasma generator nozzle; $r_1 = 4$ mm and $r_2 = 17.5$ mm.

The tests included 1) testing of the balance measurement system using a sharp cone model, 2) balance measurements of model drag, 3) pressure measurements on the model surface and inside the model, 4) video filming of the flow pattern with the plasma generator operating, and 5) schlieren pictures of the flow.

Balance and Pressure Measurement Apparatus

The drag force of the model was measured using a strain-gauge, one-component balance with a range of force measurement of 0–100 N. The balance was calibrated after each change of the model position in the test section of the T-325 wind tunnel.

The value of the model drag obtained from a strain-gauge balance accounted for the internal pressure in the model using the formula

$$N = B + \int_{r_1}^{r_2} 2\pi r P_{\text{in}}(r)\, \mathrm{d}r$$

where B is the force measured by the strain-gauge balance, r_1 is the internal radius of truncation, r_2 is the internal radius of the model forebody (Fig. 1), and $P_{\text{in}}(r)$ is the pressure distribution over the internal surface of the forebody.

The pressure distributions on the surface of the model were measured with the taps (diameter 0.7 mm) and strain gauges. These were isolated from the electromagnetic fields of the plasma generator.

Experimental Results

The plasma generator was activated when the desired wind-tunnel flow conditions were established. Plasma generator ignition resulted in a glow enveloping the model and highlighting the flowfield. Two steady flow modes were observed: short jet penetration mode (SPM) into the incoming airflow and long jet penetration mode (LPM). Both modes of flow were observed in the same experiment. The transition from one mode to another was accompanied by transient phenomena, giving different flow patterns. During these transition regimes, a reorganization of the flow structure occurred from one exhibiting a multibarreled jet structure, characteristic of the LPM, to one with one barrel, intrinsic to the SPM. Qualitatively, such phenomena have been previously observed for nonplasma counterflow cold jets embedded in supersonic flows.

Figures 2 show typical schlieren images associated with these experiments exhibiting the aforementioned features. All occur sequentially in one run at nominal, nearly constant wind-tunnel conditions with growing pressure in the plasma generator prechamber. The LPM occurred at the beginning of experiment. Then it transformed itself into the SPM. Following Refs. 8 and 10, the occurrence of the two modes was correlated with the stagnation pressure ratio parameter $P = p_{0j}/p'_{0f}$, where p_{0j} is the total pressure of a plasma jet and p'_{0f} is the total pressure behind normal shock. Figure 2a corresponds to the LPM, where $P = 3.8$. The head bow shock and trailing shocks are obvious. Figure 2c shows the SPM, where $P = 5.0$. An example of a transitional regime, $P = 4.4$, is shown in Fig. 2b. The images of both modes (exposure time $\sim$0.01 s) are superimposed in Fig. 2b. A transitional regime exhibiting instability in the zone of interaction of the jet and counterflow was observed in the range $4.1 < P < 4.5$. It is possible to estimate the critical P for which mode transition/bifurcation occurs as approximately 4.3. This value is slightly higher than that for cold counterflow jets (P critical $\sim$3) in similar flow conditions.[8] The disparity may be related to plasma effects.[18]

SPM also appears for $P < 2$. The drag force of the truncated cone model with counterflow plasma jet injection was compared with the value of the drag force of a sharp cone model. Figure 3 shows the values of the drag coefficient of the model $C_D = X/qS$, where X is the drag force of the model, q is the freestream dynamic pressure, and S is the area of model cross section, for various stagnation pressures of the flow p_{0f}, obtained by balance measurements.

Precision of the q_∞ determination was $\pm 0.5\%$. The pressure gauges had a 100-kPa measurement range, also subject to an error of $\pm 0.5\%$. Total error for C_D was ± 1–2%. The maximum error is shown as an I bar in Fig. 3 (upper right point). Because the flow under study was unsteady and the model surface was subjected to the high-temperature plasma jet, additional errors could occur due to

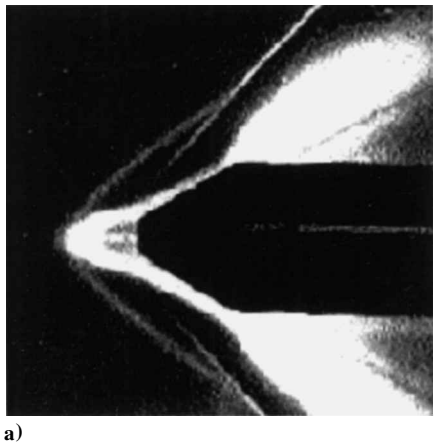

a)

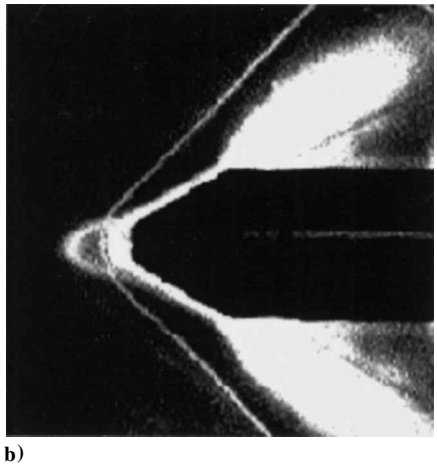

b)

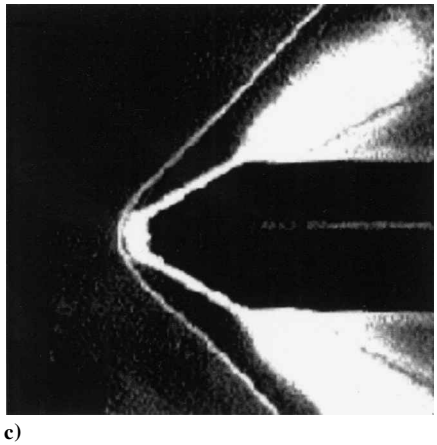

c)

Fig. 2 SPM to LPM transitions.

model erosion. Baseline experiments were carried out with a sharp cone (points 1) and blunted cone without a jet (points 2) and with a plasma jet (points 3 and 4) at $M_\infty = 2$.

Surprisingly, the sharp cone has the greatest drag for the investigated range of T-325 freestream pressures. The blunted cone has somewhat less drag. This is due to a suction force on a flat nose, even without the jet.[19] This was not measured in our experiments.

Addition of the plasma jet reduced the drag of the model. The experimental data form two groups of points corresponding to the SPM and the LPM. LPM produced the greatest drag reduction (up to 23%), whereas the drag reduction was not too significant for SPM. For the LPM, the jet penetrates much further into the flow, reducing the effective cone angle/body thickness ratio. Figure 4 shows a plot of the model drag vs the Mach number M_∞, for $p_{0f} = 100$, 200, and 300 kPa, where 1 refers to a sharp cone, 2 a truncated cone without the jet, and 3 a truncated cone with the jet. The forebody drag was estimated by integration of the measured pressure distributions, accounting for the jet thrust.

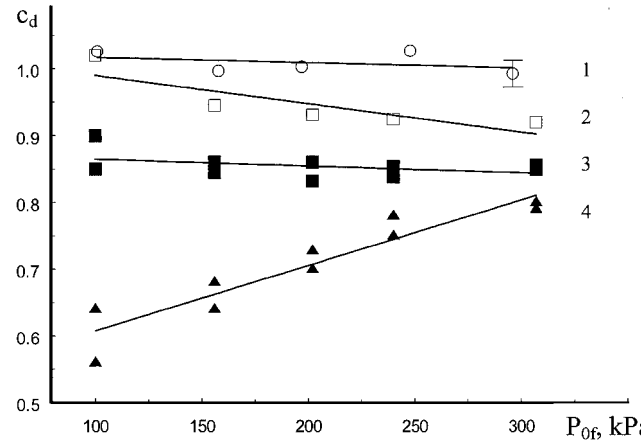

Fig. 3 Cone drag dependence on total pressure P_{0f}: 1, sharp cone; 2, truncated cone without the jet; 3, truncated cone with the plama jet, SPM; and 4, truncated cone with the plasma jet, LPM.

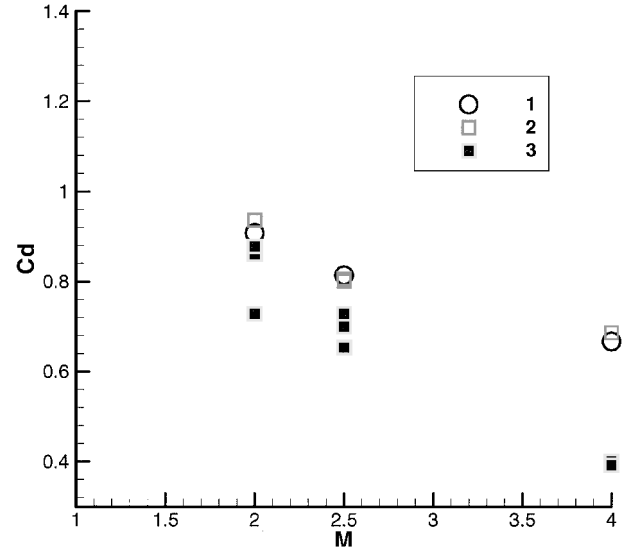

Fig. 4 Model drag dependence on freestream Mach number: 1, sharp cone; 2, truncated cone without the jet; and 3, truncated cone with the plasma jet.

Drag coefficients are plotted vs the freestream total pressure for Mach numbers $M_\infty = 2.0$, 2.5, and 4.0 and for the flow with a jet and without the jet in Fig. 5.

The forces obtained from balance and pressure measurements ($M_\infty = 2.0$) with and without the plasma jet are compared in Fig. 6. It is evident that the integrated surface pressure distribution, accounting for the internal model pressure, agrees well with the balance measured forces. This is a mutual validation of our force and pressure measurements.

Computational Studies

As another check of the experiments, a perfect gas model of the flow was implemented computationally. For the comparisons, the governing equations are the inviscid three-dimensional Euler equations for a perfect gas in conservative form. The interaction of the plasma jet with the external flow was modeled by assuming flow variable values such as Mach number and temperature at an internal boundary inside the outer far-field computational domain corresponding to the jet exit boundary. Currently, we are generalizing this model to simulate computationally the interaction of the internal nozzle and external flowfields, including plasma processes.[20]

The gas flow was considered as unsteady with a prescribed initial state. A time-explicit, space-implicit, second-order accurate, central-difference scheme with relaxation smoothing for solving the three-dimensional Euler equations by the finite volume method was used. To obtain a steady-state solution, a time-asymptotic method

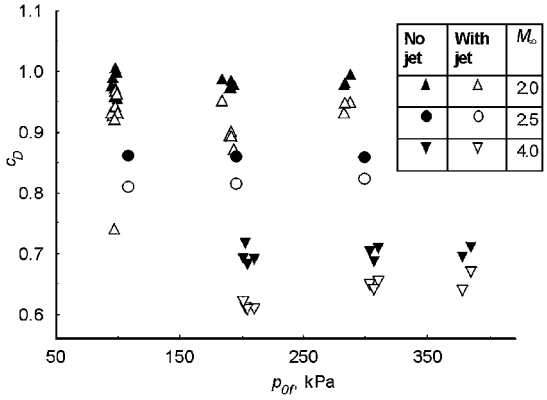

Fig. 5 Drag dependence on total pressure (pressure measurement).

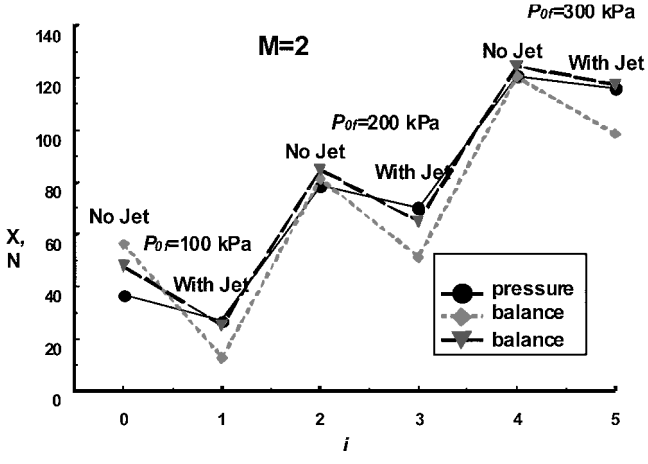

Fig. 6 Drag dependence on total pressure (pressure and balance measurement).

and a shock-capturing weakly nonmonotonic and fully conservative technique was employed. The solutions belong to the class of bounded functions.

For generation of computational grids, the algebraic method of construction of grids[21] was applied. Grid convergence was assessed from calculations on different grids (50×50, 50×100, 50×150, 100×50, 100×100, and 150×150) involving various grid densities on the bodies and in the flow. Global features of the flow solution were preserved on grid refinement but with emergence of subtle local flow details.

Comparison with Experiment

To compare the numerical and experimental data and to analyze the results obtained, a supersonic flow around a truncated cone with a counterflow jet was calculated. The truncated cone parameters were cone half-angle $\Theta_c = 30$ deg, ratio of the midsection diameter d_3 to the front face diameter d_2 of 5:1, and $d_1{:}d_2 = 1{:}4$. The freestream conditions were Mach number $M_\infty = 2$, angle of attack $\alpha = 0$, and total temperature $T_{0f} = 283$ K. The Mach number M_{aj} at the jet exit was unity. A specific heat ratio $\gamma = c_p/c_v = 1.4$ was assumed in all calculations. The parameter $P = p_{0j}/p'_{0f}$ was varied in the range 1.15–5. Total temperature in the jet was $T_{0j} = 5000$ K. These parameters were approximately typical of all of the experiments. Both modes (LPM and SPM) were obtained in the calculations.

CFD isotherms of the LPM and the SPM validating those obtained in the experiments are shown in Fig. 7. In Fig. 8, the normalized pressure $C_p = p/2q$, where p is the surface pressure on the model, for $1.7 \le P \le 4.5$ is plotted against the dimensionless coordinate X/d_2, where $d_2 = 9$ mm, for the Mach number $M_\infty = 2$ and $p_{0f} = 1$ atm. Points 1 correspond to a flow regime without a jet and points 2 and 3 with a jet in SPM and LPM, respectively. In Fig. 8, the position of the cone frustum cylinder shoulder is designated by l. The two modes are again evident. In both cases, a significant pressure change due

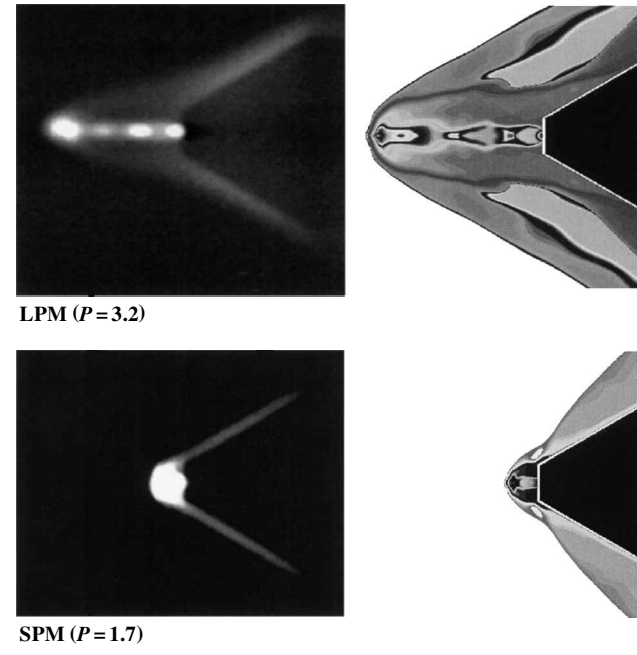

Fig. 7 Photographs and calculated isotherms of flow.

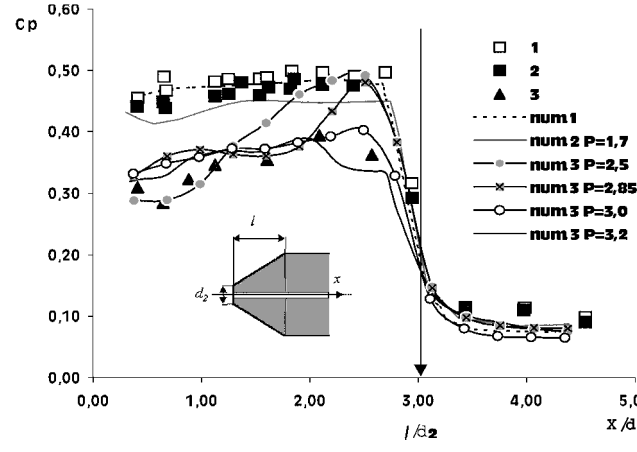

Fig. 8 Pressure distributions over conical and cylindrical surface: 1, truncated cone without a jet and 2 and 3, truncated cone with the plasma jet, SPM and LPM.

to the plasma jet occurs on the model's conical surface. A value of $P = 3.2$ provided the best CFD fit of the lower solid triangle (LPM) experimental points, although a closer estimate for P was 2.4. The value of $P = 1.7$ was used for the upper SPM group. These two cases are shown in Fig. 7. [The parameter P was obtained from experimentally measured pressures in the plasma generator chamber (giving p_{0j}) and the normal shock relations, (giving p'_{0f}).]

Uncertainty in estimating P is due to a combination of many factors. These include the time variation of the pressure in the plasma generator, adequacy of assuming choked conditions at the jet exit, heat addition in the nozzle chamber, losses in the conversion of electrical energy into kinetic energy in the nozzle, plasma effects inside and outside the nozzle, and viscous interactions such as shear layers and separations. Separate measurements are needed to assess the plasma generator efficiency. In addition, our previously mentioned more accurate simulation modeling the coupling of the internal and external flows in the numerics will be used to improve the simulation. Moreover, coupling with plasma chemistry in the high-temperature zones inside the nozzle and the core of the jet needs to be accounted for. Despite the need for such refinements, it is remarkable that the complete pressure distribution is so well reproduced with a reasonable average value for P, even on a relative basis. Absolute levels will require inclusion of plasma effects, examples of which have been cited earlier herein.

Agreement of the perfect gas Euler CFD pressure distributions with the measurements at selective flow conditions such as Mach 2 strongly suggests much of the physics at that Mach number resembles conventional (nonplasma) counterflow jet gasdynamics. The validated pressure distributions such as those obtained in this investigation (for the first time to our knowledge for plasma jets) are more convincing than drag measurements in making this assertion. The proposition that, if pressure distributions of the plasma jet flow are close to the conventional jet flow, plasma effects are insignificant is not axiomatically proven here. However, evidence of the truth of this proposition is the similarity of the observed and computed flow patterns obtained in this study, as shown in Figs. 6 and 7. Both indications suggest that this conclusion is at least one, but not a unique, possibility. Mathematically, if the pressure distribution is prescribed in the classical inverse problem of gasdynamics, and if certain side conditions such as closure for an airfoil are also given, a unique solution for the body shape and resulting flowfield is obtained. A similar statement can be conjectured for a body of revolution if a single set of governing equations of motion is used to model the flow. On the other hand, if the form of the equations of motion can be allowed to vary from conventional gasdynamics to real gas plasma gasdynamics, then this conclusion, although plausible, may be challenging to prove. To summarize, coincidence of the pressures for the plasma jet flow with those of a perfect gas jet is a necessary but not sufficient condition to assert that the two flows are equivalent. However, the resemblence of the flow patterns of the computations with those observed makes this conclusion plausible.

Although comparisons of drag between plasma and conventional counterflow jets is less convincing to arrive at such a conclusion, because they contain less information, they are an important check on the pressure measurements and useful to assess the energetic efficiency of possible drag reductions with plasma counterflow jets. These observations are major findings of this investigation. In other experiments conducted by the authors at Mach 6 and not discussed in this paper, some qualitative but less quantitative similarity is evident, and our conjecture is that plasma physics accordingly plays a more significant role. In Fig. 9, the total drag of the body

$$C_D = \left(2\pi \cdot \int_0^{d_3/2} p \cdot y \cdot \mathrm{d}y + 2\pi \cdot \int_0^{d_1/2} \rho_a \cdot v_a^2 \cdot y \cdot \mathrm{d}y \right) \Big/ q \cdot S$$

as a function of $n = p_{0j}/p_\infty$ is shown, where v_a and ρ_a are the velocity and the density in the jet exit, respectively. Here, the total drag of the body is understood to be the pressure drag plus the reaction force of the counterflow jet.

As indicated earlier, the calculations and experiments confirm the existence of the LPM and SPM configurations. The appearance of these regimes depends mainly on the pressure ratio P. Plasma effects, temperature, geometry, and perhaps other factors may be significant but have not yet been studied. LPM has appeared in the range $2 < P < 4.5$ in our studies. Outside this range, SPM was observed.

The main features of these configurations that were deduced primarily from Euler computations performed in this investigation are as follows:

1) For the SPM mode, the underexpanded jet forms a new body that moves upstream of the jetless bow shock and forms a single cell, as shown in Fig. 10. Conventional perfect gas nonplasma counterflow jets exhibiting this behavior have been previously studied.[8]

2) For the LPM mode, for some range of the pressure ratio P, the jet is compressed, and its cross section is decreased. It penetrates the jetless bow shock and forms the multicellular structure shown in Fig. 11. In this structure, a few small toroidal vortices are evident. Penetration may be relatively short or long. When the penetration is intermediate, suction, which is observed on the side surfaces of the body, can be significant. Long penetration and overblowing for a slender jet does not lead to significant decrease of the pressure on the side surfaces of the body. Here, the aerospike or long penetration jet is too far upstream and is of such high fineness ratio that it cannot significantly slenderize the body because its shock pattern is very weak and oblique and has a negligible attenuation of the jetless blunt-body bow shock system. Accordingly, an optimal range of parameters exists that maximizes drag decrease.

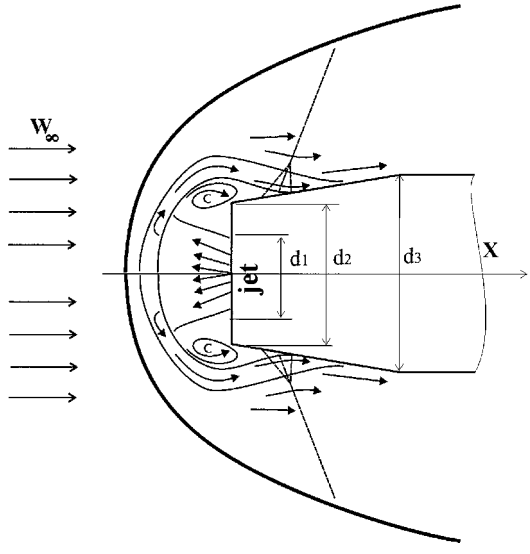

Fig. 10 Counterflow jet flow pattern: SPM.

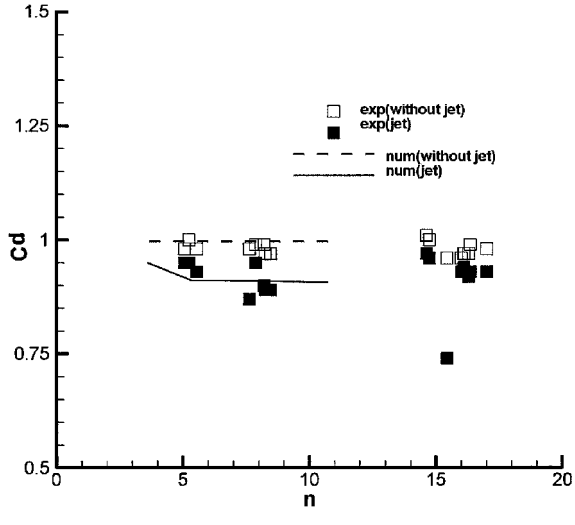

Fig. 9 Influence of the jet pressure ratio on total body drag.

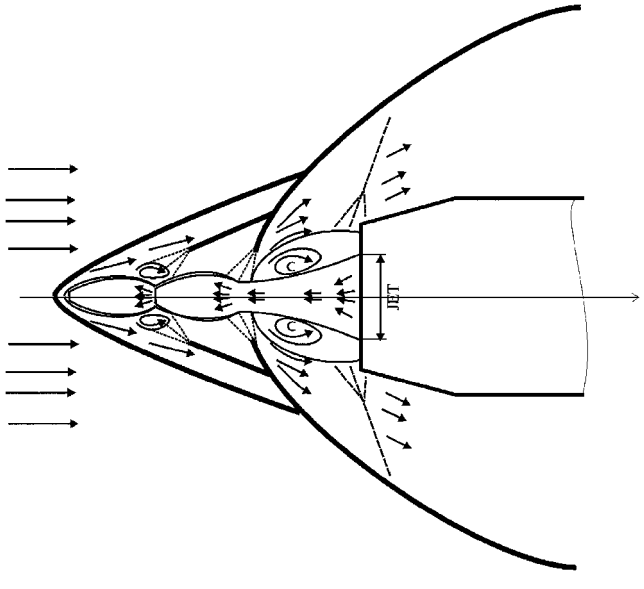

Fig. 11 Counterflow jet flow pattern: LPM.

The efficiency of plasma jet ejection in reducing drag may be estimated by comparing drag power to input power. Thus,

$$\eta = \Delta C_D \cdot q \cdot S \cdot V / Q_j$$

where ΔC_D is the reduction in drag coefficient due to the plasma jet from the value for the same body with the plasma jet off, q is the freestream dynamic pressure, S is the frontal area of the model, V is the freestream velocity, and Q_j is the electrical power used to develop plasma jet.

The value of η has been calculated for the tests discussed herein. At a freestream stagnation pressure of 1 atm, the LPM jet gave $\eta = 1.98$. For the SPM, this parameter was 0.5. This conclusively demonstrates the drag benefits of the LPM configuration. With flight-weight plasma generator units, this gain can be translated into more efficient drag reduction of hypersonic cruise vehicles such as blunted shapes for which the nose pressure drag is a dominant part of the drag buildup. Such drag reductions could have a substantial impact on aerodynamic efficiency (L/D) and result in higher payloads as well as reduced mission cost.

Qualitative Interpretations and Trends

Our calculations give trends similar to those observed by Romeo and Sterret[22,23] for cold jets. They show bifurcations as well as qualitative details of the observed flow patterns reported by these authors.

For counterflow jets, the jet specific impulse (per area unit) is higher than the impulse in the external stream downstream of the normal shock wave. This consideration suggests as a governing parameter $P = P_{0j}/P'_{0f}$, which occurs in our calculations, where P_{0j} is the stagnation pressure in the jet and P'_{0j} is the stagnation pressure downstream of the normal shock wave.

SPM and LPM Regimes

The role of jet exit Mach number and temperature, as well as the ratio of nozzle to rim diameters, will be suppressed in this part of the discussion. (In all of our calculations, this ratio was assumed to be in the range 0.2–0.25.)

Although SPM and LPM are the major modes, transitional regimes between these modes also exist. In particular, our experiments indicate different SPM regimes as shown in Fig. 12, which is also a validation of our computational model against experimental data for prediction of jet penetration and drag. We conjecture that these regimes are affected by P.

For low momentum of the jet compared to that behind the shock, SPM occurs. Here, the counterflow jet forms a reverse-circulation region whose slip line/shear layer reattaches on the side surface (Fig. 10).

An LPM regime forms when part of the jet is supersonic with a stable multibarrel shock structure. This can occur when the jet has sufficiently high momentum compared to that of the flow behind the normal shock. In this regime, the jet penetrates the flow ahead of the bow shock wave of the body with the jet off (jetless case). This creates a new oblique shock structure ahead of the bow shock that is altered from the jetless case. Our calculations suggest that a necessary condition for this regime's stability is reattachment of the eddy slip line on the rim face in contrast to its conical or cylindrical surfaces. The jet seems to be associated with a toroidal vortex and almost constant pressure inside the reverse-circulation region shown in Fig. 11. In our calculations, existence of this eddy is connected with the bifurcation of the flow at the reattachment point. These remarks pertain to the case considered in this study in which the jet diameter is small compared to the front face diameter. This case contrasts to that considered by Romeo and Sterret,[22,23] where the jet and frontal diameters are nearly the same and the rim is small.

From the computations, one can see that the attachment point can move along the flat face containing the jet exit. As soon as the attachment point migrates to the side surface, the pressure in the recirculation zone decreases. This causes a decrease in size of this zone and, correspondingly, in attachment point migration back to its original position on the flat face. This bistable equilibrium is subsequently recycled into an oscillation unless a trigger such as a downstream pressure perturbation disrupts it. If the jet becomes strongly underexpanded, the flow may transition directly to SPM. As a rule, the oscillation of the attachment point position near the boundary of the flat face causes LPM perturbations involving periodic changes of its structure and length. Although opportunities for these oscillations to occur, the LPM can be quite stable, as shown in Fig. 12. These movie stills from our tests show high dynamic stability of the jet in the LPM mode from an initial transient. This stability has practical implications for drag reduction practical application on blunt hypersonic vehicles where the forebody drag can have a major impact on payload.

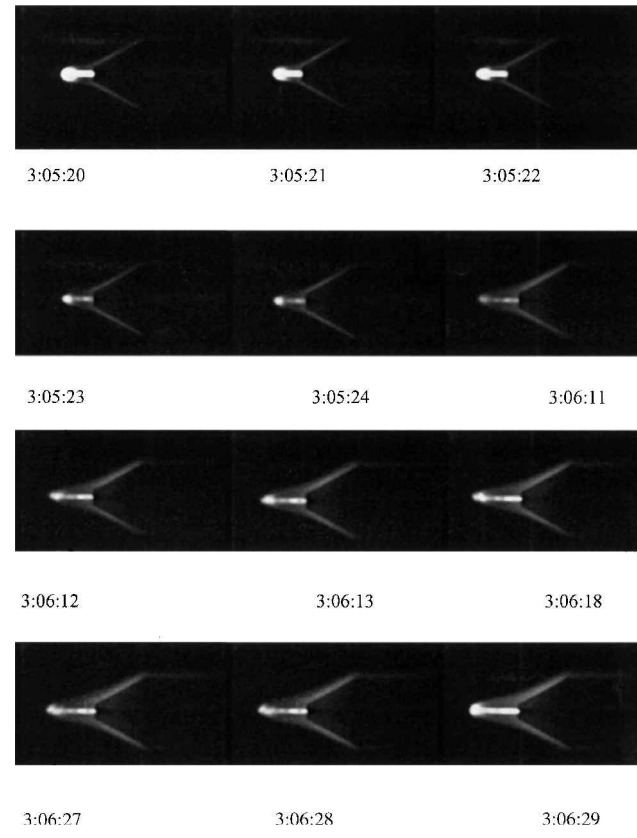

Fig. 12 Movie stills of LPM mode.

For high P (strongly underexpanded jet), a single SPM shock forms again, in contrast to the split LPM configuration.

Jet Exit Mach Number Effects

The following discussion is based on our experiments and calculations.

$M_a > 1$

If the counterflow jet is supersonic and weakly underexpanded or overexpanded at the nozzle exit, multiple cells can arise. A weakly underexpanded jet exhibits small area changes along its length. Some perturbations cause Mach number increases with reduced pressure and shrinkage of the jet. This causes its specific impulse to grow, giving increased penetration. Strongly underexpanded jets exhibit substantial area increase, resulting in a specific impulse decrease, producing a shock wave upstream of the jet. If the impulse decreases still further, the flow reverts to the SPM regime. If the supersonic jet is weakly overexpanded, its cross section decreases. This leads to an increased specific impulse and an LPM configuration. Strongly overexpanded jets create a normal shock with a decreased specific impulse that leads to SPM.

$M_a = 1$

For sonic jets, supersonic and subsonic conditions can occur upstream of the jet similar to Laval nozzle flow. A weakly underexpanded jet can expand, giving supersonic flow. This leads to LPM. SPM can occur for strongly underexpanded or overexpanded jets.

$M_a < 1$

Here, the LPM regime can be associated with a convergent lip angle with acceleration to critical conditions and an upstream throat and farther upstream behavior already discussed for the choked case. We have observed this behavior in our computations but only for high-temperature experiments.

To summarize, LPM flow in our calculations was observed for supersonic jets whose pressure differs little from the external jet pressure. It is not very important whether the nozzle exit is subsonic, sonic, or supersonic. If conditions exist for a supersonic transition and the jet is generally weakly underexpanded, LPM can occur. These are necessary but insufficient conditions. An associated vortex seems also to be a feature of this flow.

Effects of Separation

Some interesting studies that are useful in understanding the effect of the separated region in the LPM mode stem from the work of Ehrich,[24] who extended the Zhukovski hodograph method discussed by Milne-Thompson[25] to infinite slot two-dimensional (planar) jets in a crossflow. The closed-form solutions in Ref. 24 include counterflow jets as a special case. For the latter, penetration was limited if the flow was attached to the outside of the slot. In contrast, the penetration became infinite at a finite jet-to-freestream velocity ratio if the jet was separated over the slot. These effects are relevant to the discussion herein as well as those in Refs. 26 and 27.

Summary

Results of experimental and numerical studies of the influence of a thin counterflow, high-temperature jet on the aerodynamic characteristics of a blunted body in supersonic flow have been presented.

The experiments were conducted with plasma jet injection into supersonic and low hypersonic freestreams. They included balance, pressure distribution measurements, video and photographic visualization, and schlieren pictures. Two stable regimes of the plasma jet flow resembling ordinary perfect gas counterflow jets were found. These are SPM and LPM into the freestream. LPM produced the only substantial drag reduction, which was especially strong for transition from SPM to LPM.

Experimental pressure distributions over the surface of a truncated cone–cylinder model in the presence of a plasma jet were obtained. These distributions represent the first data of this type for onboard plasma jets and should be useful for separating aerodynamic heating from plasma physics phenomena in aerodynamic augmentation.

The experimental results were compared to Euler perfect-gas, hot-jet CFD models. Both SPM and LPM were obtained with these simulations. On the basis of our calculations, we believe that the bifurcation is driven by interaction of separated flow regions and the delicate role of reattachment points that interact with the flow and shock system on a global scale. These can be driven by the nozzle cavity flow and oscillations from the plasma generator. From a different perspective, we believe that the bifurcation is related to a nonuniqueness of the steady-state boundary value problem for the gasdynamic equations of motion, which may be an eigenproblem in a bifurcation stability sense. This indeterminacy relates to the classical incompressible problem of oblique collision of jets, which is nonunique to within an unknown constant. This nonuniquenessis related to the need to incorporate the flow history through determinism to assess the current state of the colliding jet flow. In this connection, conventional time-marching CFD codes may give path-dependent solutions rather than unique time asymptotics, due to a number of factors including stability of the temporal solution that might be an asymptotically bistable oscillation between the bifurcation SPM and LPM modes. We have correlated the LPM–SPM switch to a change in the position of the reattachment. We noticed migration of the attachment point from the forward face containing the jet exit to the inclined face and correlated this with LPM and SPM.

The numerical results are in reasonable agreement with the experimental data for supersonic freestreams, for both pressure distributions and drag, if the key stagnation pressure parameter P was adjusted within the experimentally observed range. This suggests that the dominant physics is fluid dynamics and that the plasma effects are relatively small at moderate supersonic Mach numbers. In particular, the large drag reductions associated with the LPM result from the resulting suction on the forward facing parts of the cone cylinder, namely, the conical face. Nevertheless, aerodynamic heating that controls much of the moderate Mach number flow has an important link to plasma processes, which are the only means of producing the intense energy densities and high temperatures in the plasma jet. These temperatures can be several thousand degrees Kelvin higher than those of conventionally heated jets. For hypersonic cases, the agreement of calculation and experimental results is only qualitative. We believe that this uncertainty is partly caused by plasma effects that were not taken into account. Future work will be focused on this aspect.

Acknowledgments

The financial support of The Boeing Company and Rockwell Scientific Company is acknowledged. Portions of this effort were also supported by the Air Force Office of Scientific Research, Air Force Materials Command, under Contracts F49620-92-C-0006and F49620-96-C-0004. The authors thank A. N. Timoshevsky for advice on the plasma generator, A. A. Pavlov for advice on optical measurement, and B. V. Postnikov and B. A. Pozdniakov for preparation of the equipment and participation in the experiments. The U.S. Government is authorized to reproduce and distribute reprints for government purposes, notwithstanding any copyright notation thereon. The views and conclusions herein are those of the authors and should not be interpreted as necessarily representing the official policies or endorsements, either expressed, or implied of the Air Force Office of Scientific Research or the U.S. Government.

References

[1]Aradailov, S. I., "Influence of Energy Output in a Shock Layer on Supersonic Flight of Bodies," *Izvestiya Akademii Nauk SSSR, Mekhanika Zhidkosti i Gasa*, No. 4, 1987, pp. 178–184 (in Russian).

[2]Bazhenova, T. V., Lyakhov, V. N., Pankova, M. B., and Kharitonov, S. M., "Numerical Simulation of a Thermal Non-uniformity in a Supersonic Flow on a Drag Coefficient of a Spherical Body," *Chislennoe Modelirovanie Nestatsionarnykh Gazodinamicheskikh i MGD Techenii*, IVTAN, Moscow, 1989 (in Russian), pp. 53–64.

[3]Bergelson, V. I., Mcdvedyuk, S. A., Nemchinov, I. V., Orlova, T. I., and Hazins, V. M., "Aerodynamic Characteristics of a Body at Various Localization of a Thermal Needle," *Matematicheskoe Modelirovanie*, Vol. 8, No. l, 1996, pp. 3–10 (in Russian).

[4]Borzov, V. Y., Rybka, I. V., and Yurev, A. S., "Influence of the Local Energy Input in a Hypersonic Flow on Drag of Bodies with Various Bluntness," *Inzhenerno-Fizicheskii Zhurnal*, Vol. 67, No. 5, 1994, pp. 355–361 (in Russian).

[5]Chernyi, G. G., "The Impact of Electromagnetic Energy Addition to Air Near the Flying Body on its Aerodynamic Characteristics," *Proceedings of Weakly Ionized Gas Workshop*, AIAA, Reston, VA, 1998, pp. 1–20.

[6]Tretyakov, P. K., Fomin, V. M., and Yakovlev, V. I., "New Principles of Control of Aerophysical Processes Research Development," *Proceedings ICMAR-96*, Pt. 2, Inst. of Theoretical and Applied Mechanics, Novosibirsk, Russia, 1996, pp. 210–220.

[7]Fomin, V. M., Lebedev, A. V., and Ivanchenko, A. I., "Speckle Photography of Turbulence Variation After Shock Wave Passage," *Proceedings ICMAR-98*, Pt. 2, Inst. of Theoretical and Applied Mechanics, Novosibirsk, Russia, 1998, pp. 54–56.

[8]Finley, P. J., "The Flow of a Jet From a Body Opposing a Supersonic Free Stream," *Journal of Fluid Mechanics*, Vol. 26, Pt. 2, 1966, pp. 337–368.

[9]Kalinin, V. M., and Melbardt, A. M., "Parameters of Simulation in a Problem of the Supersonic Unexpanded Jet Efflux Forward to a Supersonic Flow," *Izvestia Akademii Nauk SSSR, Mekhanika Zhidkosti i Gasa*, No. 3, 1980, pp. 83–89 (in Russian).

[10]Yudintsev, Y. N., and Chirkashenko, V. F., "Interaction Regimes in a Counterflow Jet with a Supersonic Flow," *Gasodinamika I Acustica Struinyh Techenii*, Inst. of Theoretical and Applied Mechanics, Novosibirsk, Russia, 1979, pp. 75–106 (in Russian).

[11]Zhirikov, B. L., and Petrov, K. P., "Research of Interaction of Jets with a Counter Flow Flowing from a Frontal Surface of a Body of Revolution," *Sovremennye Problemy Aerodinamiki*, Machinostroenie, Moscow, 1987, pp. 114–122 (in Russian).

[12]Ganiev, Y. C., Gordeev, V. P., Krasilnikov, A. V., Lagutin, V. I., and Otmennikov, V. N., "Experimental Study of the Possibility of Reducing Aerodynamic Drag by Employing Plasma Injection," *Proceedings Third International Conference on Experimental Fluid Mechanics*, TsNIIMash, Korolev, Moscow Region, Russia, 1997, pp.1–6.

[13]Klimov, A., "Anomalous Supersonic Flow and Shock Wave Structure in Weakly Ionized Plasmas," *Proceedings 1st Workshop on Weakly Ionized Gases*, U.S. Air Force Academy, CO, 1997, pp. 1–20.

[14]Leonov, S., "Experiments on Influence of Plasma Jet Lift and Drag of Wing," *Proceedings 1st Workshop on Weakly Ionized Gases*, U.S. Air Force Academy, CO, 1997, pp. 1–24.

[15]Fomin, V. M., Maslov, A. A., Malmuth, N. D., Fomichev, V. P., Shashkin, A. P., Korotaeva, T. A., Shiplyuk, A. N., and Pozdnyakov, G. A., "Influence of a Counterflow Plasma Jet on Supersonic Blunt-Body Pressures," AIAA Paper 99-4883, Nov. 1999.

[16]Hornung, H. G., "The Forebody Drag of a Cone with a Counterflow Jet in Supersonic Flow," GALCIT Rept. 97-20, California Inst. of Technology, Pasadena, CA, 1997.

[17]Shang, J. S., Hayes, J., and Menart, J., "Hypersonic Flow over a Blunt Body with Plasma Injection," AIAA Paper 2001-0344, Jan. 2001.

[18]Lukianov, G. A., *Supersonic Plasma Jet*, Mashinoctroenic, Moscow, 1985 (in Russian).

[19]Chernyi, G. G., "High Velocity Supersonic Flow," *Fizmatlit*, 1959 (in Russian).

[20]Ardelyan, N., Bychkov, V., Kosmachevskii, K., Chuvashev, S., and Malmuth, N., "Modeling of a Plasma Generator for Electron Beam and Plasma Jet Aerodynamic Applications," AIAA Paper 2001-3101, June 2001.

[21]Korotaeva, T. A., Rakhimov, R. D., and Shashkin, A. P., "Computational Mesh Construction for Numerical Analysis of Three-Dimensional Supersonic Flow over Two Bodies," *Thermophysics and Aeromechanics*, Vol. 3, No. 3, 1996, pp. 203–212.

[22]Romeo, D. J., and Sterret, J. R., "Exploratory Investigation of a Forward-Facing Jet on the Bow Shock of a Blunt Body in a Mach 6 Free Stream," NASA TN D-1605, Feb. 1963.

[23]Romeo, D. J., and Sterret, J. R., "Flowfield for Sonic Jet Exhausting Counter to Hypersonic Mainstream," *AIAA Journal*, Vol. 3, No. 3, 1965, pp. 544–546.

[24]Ehrich, F., "Penetration and Deflection of Jets Oblique to a General Stream," *Journal of the Aeronautical Sciences*, Feb. 1953, pp. 99–104.

[25]Milne-Thompson, L. M., *Theoretical Hydrodynamics*, 4th ed., Macmillan, New York, 1960, pp. 283–294.

[26]Fomin, V. M., Maslov, A. A., and Malmuth, N. D., "Experimental Investigation of Counterflow Plasma Jet in Front of Blunted Body for High Mach Number Flows," *Proceedings of the 2nd Workshop on Magneto-Plasma Aerodynamics in Aerospace Applications*," IVTAN, Moscow, 2000, pp. 112–116.

[27]Fomin, V. M., Maslov, A. A., and Malmuth, N. D., "Numerical Investigation of Counterflow Jet Penetration in Hypersonic Flow," *Proceedings of the 2nd Workshop on Magneto-Plasma Aerodynamics in Aerospace Applications*, IVTAN, Moscow, 2000, pp. 116–121.

P. Givi
Associate Editor